Monomeric bovine β-lactoglobulin adopts a β-barrel fold at pH 2

F. Fogolari[a], L. Ragona[b], L. Zetta[b], S. Romagnoli[a], K.G. De Kruif[c], H. Molinari[a,*]

[a] *Istituto Policattedra, Università degli Studi di Verona, Strada Le Grazie, 37100 Verona, Italy*
[b] *Laboratorio NMR, CNR, ICM, Via Ampere 56, 20131 Milan, Italy*
[c] *Department of Biophysical Chemistry and Technology, Netherlands Institute for Dairy Research (NIZO), 6710 BA Ede, The Netherlands*

Received 26 May 1998; revised version received 9 July 1998

Abstract We have determined a crude structure of the apo form of bovine β-lactoglobulin, a protein of 162 amino acid residues with a molecular mass of 18 kDa, at a low pH on the basis of data collected using only homonuclear ^{1}H NMR spectroscopy. An ensemble of protein conformations was calculated with the distance-geometry algorithm for NMR applications (DYANA). The monomeric protein at low pH adopts a β-barrel fold, well-superimposable on the structure determined by X-ray crystallography for the dimer at physiological pH. NMR evidence suggests the presence of disordered loop regions and terminal segments. Structural differences between the monomer at pH 2 and the dimer at pH 7, obtained by X-ray crystallography, are discussed, paying particular attention to surface electrostatic properties, in view of the high charge state of the protein at low pH.

Key words: Bovine β-lactoglobulin; Nuclear magnetic resonance; Structure calculation; Surface electrostatic property

1. Introduction

Bovine β-lactoglobulin (β-LG) is a very abundant globular milk-whey protein expressed in the glandular epithelium of the mammary gland in ruminants and some other species [1]. β-LG, a 18 kDa polypeptide, has been identified as a member of the lipocalin superfamily, a class of molecular transport proteins capable of binding small hydrophobic compounds [2]. The function of β-LG is unknown but it binds retinol and fatty acids in milk and a number of other small hydrophobic molecules in vitro. It has been postulated that β-LG could function to bind and protect retinol, or some other small hydrophobic molecule, during passage through the stomach, in order to deliver its ligand to a specific receptor reported to be located in the intestine of the suckling neonate [2,3]. The passage of the protein through the gastric tract implies the capability to maintain a functional structure at low pH; the knowledge of the structural properties of β-LG at pH 2 is therefore a relevant step towards the understanding of the function and the mechanism of transport of hydrophobic ligands.

We have previously published an NMR study of the low pH form β-LG in which we describe the identification of two clusters of hydrophobic residues present in the partially folded low pH form, and which are conserved in all the homologous proteins belonging to the lipocalin family [4,5]. We have identified and reported a large number of long-range NOE effects characterising the β-core of this molecule [4], and we report here an ab initio structure calculation, aimed at determining whether the observed NOEs define an overall crude structure similar to that found in the native state. Different experimental conditions and different genetic variants were employed for the determination of the X-ray [6] and NMR structures [4,5]. X-ray data were obtained from the commercial protein (mixture of genetic variants A/B)[1] at physiological pH, while all our NMR studies have been performed on the protein purified from milk (genetic variant B), at pH 2 and at a low ionic strength, where the protein is essentially monomeric. β-LG exhibits a complex pattern of association and aggregation under physiological conditions and its behaviour is largely influenced by pH changes; a monomer-dimer equilibrium is present above pH 3.5 [7]. The protein we purified was carefully delipidated [4], while the commercial preparations were reported to contain ca. 0.5 mol:mol of palmitic acid to protein [8,9].

Our main purpose is to understand (i) whether the NOE connectivities obtained on the monomer at pH 2 are sufficient to define the β-barrel fold as observed by X-ray crystallography in the dimer at pH 7 [6] and whether there are sizeable differences in the overall fold due to different environmental conditions; (ii) whether disordered regions observed in the low pH form [5] are localised only in terminal segments and loops or at the level of the barrel structure.

The structure calculation reported in this paper is derived from the completed ^{1}H NMR assignment of the β-barrel and of the terminal helix. This is, to the best of our knowledge, the first structural characterisation of the low pH form of β-LG. In spite of the intrinsic limitations of ^{1}H NMR spectroscopy applied to a 18 kDa protein, the resolution of our models allows the comparison of the overall topology of the low and neutral pH structures, which can shed light on the mechanism of folding, association and ligand binding and clarify the biological role of the protein.

2. Materials and methods

Bovine β-LG prepared from fresh milk was provided by NIZO (Netherlands Institute for Dairy Research). All NMR measurements were performed using a 0.9–1 mM concentration of protein in a buffer solution consisting of 12 mM H_3PO_4/NaOH and 5% D_2O (pH 2–2.1). The pH values quoted are uncorrected for isotopic effects.

^{1}H 1D and 2D NMR experiments were performed as described earlier [4,5] on Bruker spectrometers operating at 500.13 and 800.13 MHz. A series of 2D ^{1}H TOCSY [10,11] were recorded to follow the time-dependent loss of the NH resonances as the H-to-D exchange proceeded. The H_2O/D_2O exchange experiments were performed using concentration cells at low temperature (285 K) and were immediately followed by the acquisition of TOCSY spectra in D_2O at 310 K.

*Corresponding author. Fax: (39) (2) 2663030.
E-mail: henry@labnmr.icmnmr.mi.cnr.it

[1] Genetic variant A differs from B in the following: G64D and A118V.

PII: S0014-5793(98)00936-3

Successive TOCSY were repeated at different times following the exchange.

Cross-peak volumes of the 500 MHz NOESY spectra [11] at $t_m = 100$ and 160 ms were integrated using the software package Felix95 (MSI, San Diego, CA). For cross-peaks involving multiple protons (like those arising from methyl or unresolved methylene protons) we took the sixth root of the integrated volume and added a fixed amount (1 Å) to the distance. All obtained distances were multiplied by a factor of 1.1 to obtain upper bounds. For multiple protons the bound was applied to a pseudo-atom at the centre of geometry of the protons. This correction procedure is very close to the standard correction procedure depicted by Wüthrich and coworkers [12]. In all cases where a severe overlap prevented us from measuring cross-peak volumes, a distance of 4 Å was assumed between the interacting protons. All the available experimental information was used as input for the program DYANA [13]. Overall, 493 cross-peaks (198 intraresidue, 109 sequential and 186 medium and long range) were assigned and 443 of them were also integrated, which led, after the analysis of the DYANA program, to a set of 444 (123 intraresidue, 109 sequential and 212 medium and long range) meaningful distance restraints. The resolved cross-peak volumes of Trp-19 aromatic ring resonances were employed as calibrants, namely those arising from $H\delta_1$-$H\varepsilon_1$ and $H\zeta_2$-$H\varepsilon_1$ hydrogen pairs, whose dipolar interactions correspond to internuclear separations of 2.54 and 2.89 Å, respectively. This choice was adopted because Trp-19 shows the highest number of inter-residue cross-peaks among all residues of the molecule; therefore its rotational correlation time is expected to be representative of the random motions of the residues in the hydrophobic cluster, whose structure is reported in this study. Further evidence to corroborate this point comes from the observation that Trp-19 is the most conserved residue in the lipocalin family. Another reason for choosing the fixed distance among Trp-19 protons as a yardstick for deriving other distances, compared to other fixed distances such as that between methylene protons, is that it falls closer to the centre of the range of the NOESY observable distances. This should minimise the errors typically associated with this approach. Based on the availability of the $H\varepsilon_1$ auto-peak integrated intensity it was possible to estimate the rotational correlation time of the internuclear vectors, using the method of the cross-peak-to-auto-peak ratio [14]. The determined values of 6.7 and 8.4 ns were in reasonable agreement with the correlation time value of 7.8 ns for the overall molecular tumbling, estimated according to Stokes' law using an effective hydrodynamic radius value of ca. 20 Å, according to the formula reported by Cavanagh et al. [15]. As an internal check, the estimate obtained for other fixed distances was calculated, and the results obtained were in agreement with the proper values. Due to the long rotational correlation time of the molecule and the possibility of substantial spin-diffusion, only upper distance bounds were imposed. No stereospecific assignment was attempted for the same reason. Separate runs were performed on isolated structural motifs of the molecule to check for consistent violations. Since the results at this stage did not show major inconsistencies in the restraints, we did not correct any upper bounds, but deferred this task to after having performed the runs on the whole molecule. We chose to employ the simulated annealing protocol to generate structures with a low value for the variable target function [13].

We started generating 200 structures, the 10 best of which were retained, selected according to lowest values of the target function [13]. Violations of the restraints exceeding 0.2 Å were monitored. When these were found in at least 5 of the 10 best structures the corresponding restraint was relaxed by 0.5 Å. This step led to the correction of 29 upper bounds. Another 600 structures were subsequently generated and the 10 best structures were retained and further analysed. The 10 best structures had error function values ranging between 1.52 and 2.08. In all structures the maximum violation did not exceed 0.5 Å.

Electrostatic fields were calculated via numerical solutions of the Poisson-Boltzmann equation using the software package UHBD [16], and using charges and radii taken from the CHARMM forcefield [17], setting the ionic strength to 100 mM, and the internal dielectric constant to 4. Grids of $110\times110\times110$ points were used with a focusing step with a final mesh of 0.8 Å. The electrostatic potential maps were finally converted into $65\times65\times65$ point maps for visualisation with GRASP [18]. Electrostatic surfaces were visualised and analysed using the software package GRASP and InsightII (MSI, San Diego, CA).

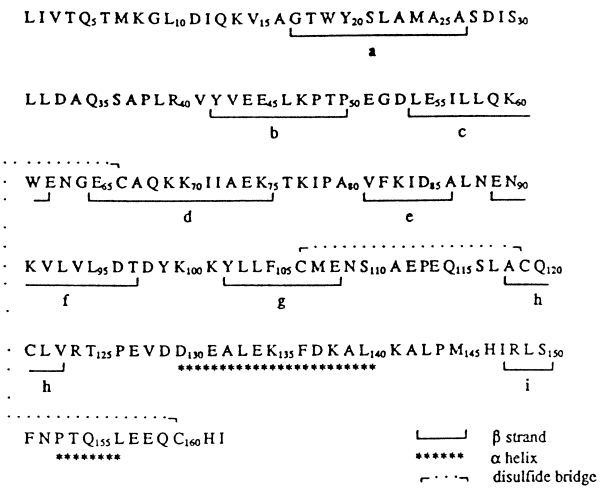

Scheme 1.

3. Results and discussion

Our previous NMR data [4,5] obtained on β-LG B at low pH and low ionic strength pointed to the simultaneous presence of an ordered globular structure and of disordered regions, as suggested by the analysis of the fingerprint zone of the TOCSY spectra. These contain well-defined cross-peaks, characterised by secondary shifts typical of β structure, and a broad overlapped region centred at the random coil value, typical of disordered segments. As mentioned before, our assignment has been entirely based on homonuclear ^{1}H NMR experiments; we have used different experimental conditions, such as variable ionic strength, temperature and amounts of NaCl to identify most of the overlapped spin systems, which moved differentially upon changing the environment. This procedure allowed us to collect additional data with respect to those reported in [4] including (i) the short *cd* loop (see Scheme 1); (ii) the first residues of the terminal helix (130–135) identified on the basis of strong $d_{NN}(i,i+1)$, weaker $d_{\alpha N}(i,i+3)$ and $d_{NN}(i,i+2)$ connectivities; (iii) the short additional strand *i* (148–150) detected on the basis of $d_{\alpha N}(i,i+1)$ and $d_{\alpha\alpha}(i,j)$ connectivities with strand *a*. The completed ^{1}H NMR assignment and the interproton distance upper bounds are provided as supplementary material.

NMR data were employed to extract internuclear distances (see Section 2), hydrogen bonds and dihedral angle restraints. We did not attempt to include any hydrogen bond restraint in our input data for structure calculation so as not to introduce any bias in the absence of a well-defined structure. J-couplings were extracted from DQF-COSY [19] spectra using the method of Kim and Prestegard [20]. The straight application of their formulas led mostly to overestimated values of the J-couplings (reported as supplementary material). Although coupling constants appeared overestimated by several Hz, the lowest constants were found in the regions 130–140 and 62–65. J-couplings were not used for structure determination but served as a useful verification on the quality of our data.

The quality of NOE derived restraints may be judged from Fig. 1, which reports a graphical representation of the restraints grouped for distances among interacting residues in the sequence and for residue number. Pairwise superposition of the backbone atoms of well-defined secondary structure

elements detected (i.e. residues 17–26, 42–48, 54–75, 81–84, 90–97, 102–108, 118–123, 130–140 and 148–151) led to an average root mean square deviation (RMSD) of 2.15 ± 0.33 Å. The plot of the backbone atoms average RMSD when the core region is superimposed and when groups of three adjacent residues are superimposed shows the structurally defined regions (Fig. 2). In particular, for residues 17–25, 43–48, 53–59, 67, 68, 72–74, 81–83, 90–96, 101–108, 118–124 and 134–137 the average RMSD is lower than 2 Å, when the pairwise superpositions are performed as described above. These residues were used to superimpose our structures with chain A of the X-ray structure [6] (Fig. 3). The result is an average RMSD of 1.8 Å, which shows that, within our resolution limits, the overall tertiary structure is conserved from the dimer at pH 7 to the monomer at pH 2. Sizeable differences are observed in the *cd* loop and flanking residues and in the positioning of the helix relative to the β-barrel. To assess whether the observed differences, occurring in *cd* loop region where the average RMSD is larger than 2 Å, are due to lack of restraints or real conformational mobility, H-D exchange experiments were performed. Residues 54–60, 69, 71, 73 and 74 do not exchange even after three weeks, while all other amides (with the exception of residue 72 which could not be resolved) in the stretch 54–75 exchange immediately or within 90 h. The exchange pattern is in line with the computed

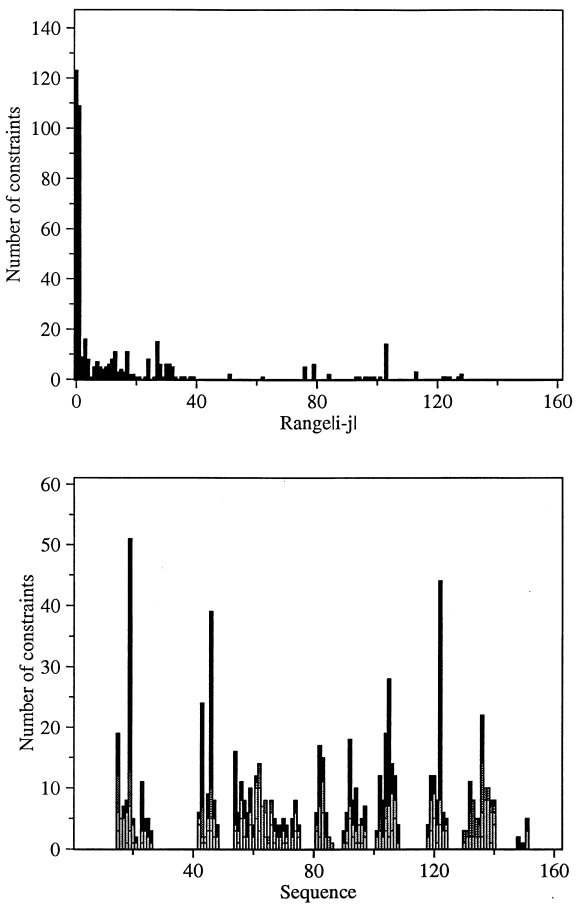

Fig. 1. Number of restraints versus the distance in the primary sequence among the interacting residues (upper panel) and versus residue number (lower panel). In the lower panel intraresidue, sequential, medium and long range restraints are shown as white, light grey, dark grey and black bars, respectively.

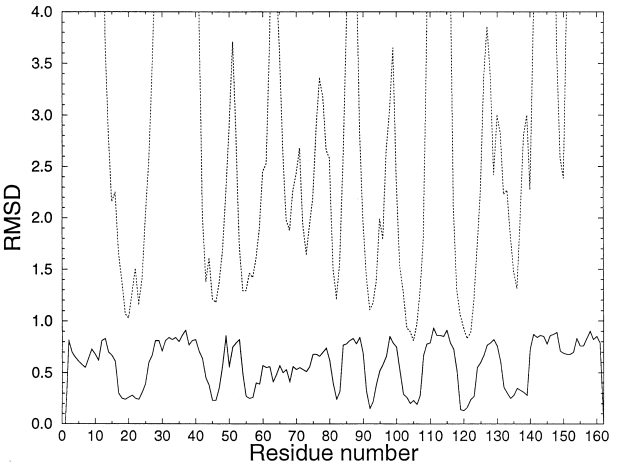

Fig. 2. The average RMSD among residue backbone atoms when backbone atoms of residues 17–26, 42–48, 54–75, 81–84, 90–97, 102–108, 118-123, 130–140 and 148–151 are superimposed (dashed line) and when only three contiguous residues are superimposed (continuous line).

RMSD and compatible with local mobility. For residues 69 and 71, notwithstanding the relatively high backbone atoms RMSD: 2.2 and 2.6 Å, respectively, hydrogen bonding was detected in 9 and 8, respectively, out of the 10 best NMR structures. Regardless of the RMSD, the conserved hydrogen bonds, which are incidentally the most consistent hydrogen bonds among residues 54–75, explain the observed H-D exchange data. It is worth noting that the *cd* loop and the flanking residues do not establish any further hydrogen bond with strands *b* and *e* neither in the NMR nor in the X-ray structure and therefore some degree of mobility should be expected. It is somewhat more difficult to discuss the differences observed in the low and neutral pH structures for the terminal α-helix positioning relative to the β-barrel contacts, since this involves non-contiguous residues [5].

The previously described hydrophobic cluster involving residues 15, 19, 43, 46, 54, 82, 92, 94, 103, 105, 122 is well-defined and the average RMSD when these residues are superimposed is 1.0 ± 0.2 Å and 1.31 ± 0.2 Å when backbone atoms and all heavy atoms, respectively, are considered for superposition. The surface hydrophobic patch involving residues 23, 102, 104, 135, 136 and 139 appears to be only loosely defined, with an average RMSD of 1.3 ± 0.6 Å and 2.2 ± 0.5 Å when backbone atoms and all heavy atoms, respectively, are considered for superposition. A loose connection between the terminal α-helix and the β-barrel could explain the different positioning of the two regions in the X-ray dimer structure and the present NMR structures. Besides H-D exchange data, support for the non-artifactual mobility in this region comes from the observation of a large shift in the amide proton chemical shifts of the residues connecting the α-helix with the β-barrel, upon mild environmental changes (see below and Fig. 4).

Terminal segments and loop regions, with the exception of the short *cd* loop, could not be assigned. However, we expect that their resonances should account for the highly overlapped region centred at the typical random coil chemical shift values. Further evidence to support this point comes from the immediate disappearance of the resonances of this region upon dissolving the protein in D_2O. All these data are con-

sistent with the high mobility of the loop regions. The emerging picture of the low pH conformation of β-LG (within our resolution limit) is therefore that of a native-like β-barrel flanked by a terminal α-helix, with disordered loops and terminal residues.

In view of the high charge state of the protein at low pH, we propose that the driving force leading to protein dissociation and loop and terminal segment mobility is mainly electrostatic. In particular, lowering the pH leads to the full protonation of the protein, resulting in a net charge of +21 proton charges. The free energy change in the process of protein monomerisation can be estimated via the old Linderstrom-Lang model [21] or via the more refined Poisson-Boltzmann approach [22] to be in the range of a few kcal/mol to some tens of kcal/mol, depending upon pH and ionic strength. This pH-dependent contribution to the free energy is eventually able, together with the entropic gain in overall and contacting side-chain translational and rotational freedom, to overcome the large opposing 'hydrophobic' free energy which keeps the dimer together at pH 7. A similar mechanism is responsible for the disordering of the loops and terminal regions in the monomer. Eleven positive charges of the protein are located in loops and terminal regions, therefore the ordered → disordered transition in these regions should significantly lower the electrostatic free energy. The overall free energy change per residue in the folding process, which is conceptually similar to the two processes discussed above, is very low and is the result of compensation of very large contributions [23]; therefore any further quantitative analysis should be very carefully performed.

We have compared the surface electrostatic properties of different models for β-LG at low and neutral pH: (i) the fully protonated form of chain A of the X-ray structure (with and without the terminal residues and the long *ab* loop, i.e. with and without residues 1–13, 27–41, 143–162), (ii) the fully protonated form of the most representative of the NMR structures and (iii) the dimer with all arginines, lysines and histidines, protonated and all aspartic and glutamic acids deprotonated. We noticed that: (i) at low pH two high potential regions could be detected for the fully protonated form of chain A of the X-ray structure, located at residues D_{98}, K_{101}, Y_{102}, E_{131}, A_{132}, K_{135} and K_{60}, K_{69}, L_{87}, i.e. in proximity of the *fg* loop-α-helix interface and of the β-barrel open end, respectively. These high surface potential areas are not changed upon terminal and *ab* loop segments removal; (ii) for the NMR representative structure, terminal and loop disordering changes the surface potential pattern, and several regions possess rather high potential. The region close to resi-

Fig. 3. The 10 best NMR structures (only the best defined residues are shown, i.e. residues 17–25, 43–48, 53–59, 67, 68, 72–74, 81–83, 90–96, 101–108, 118–124 and 134–137) superimposed on chain A of the X-ray structure, shown here as a ribbon including all well-defined secondary structure elements.

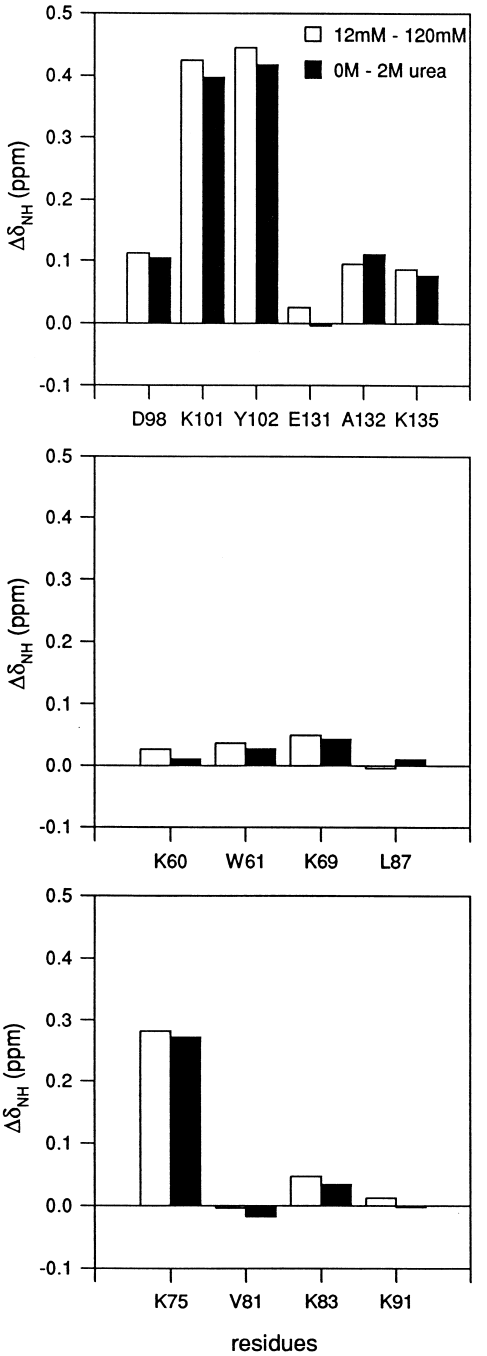

Fig. 4. Chemical shift changes observed in three high surface potential regions upon increasing the ionic strength from 12 mM to 120 mM (white bars) and upon increasing urea concentration from 0 to 2 M (black bars). Only assigned residues are reported.

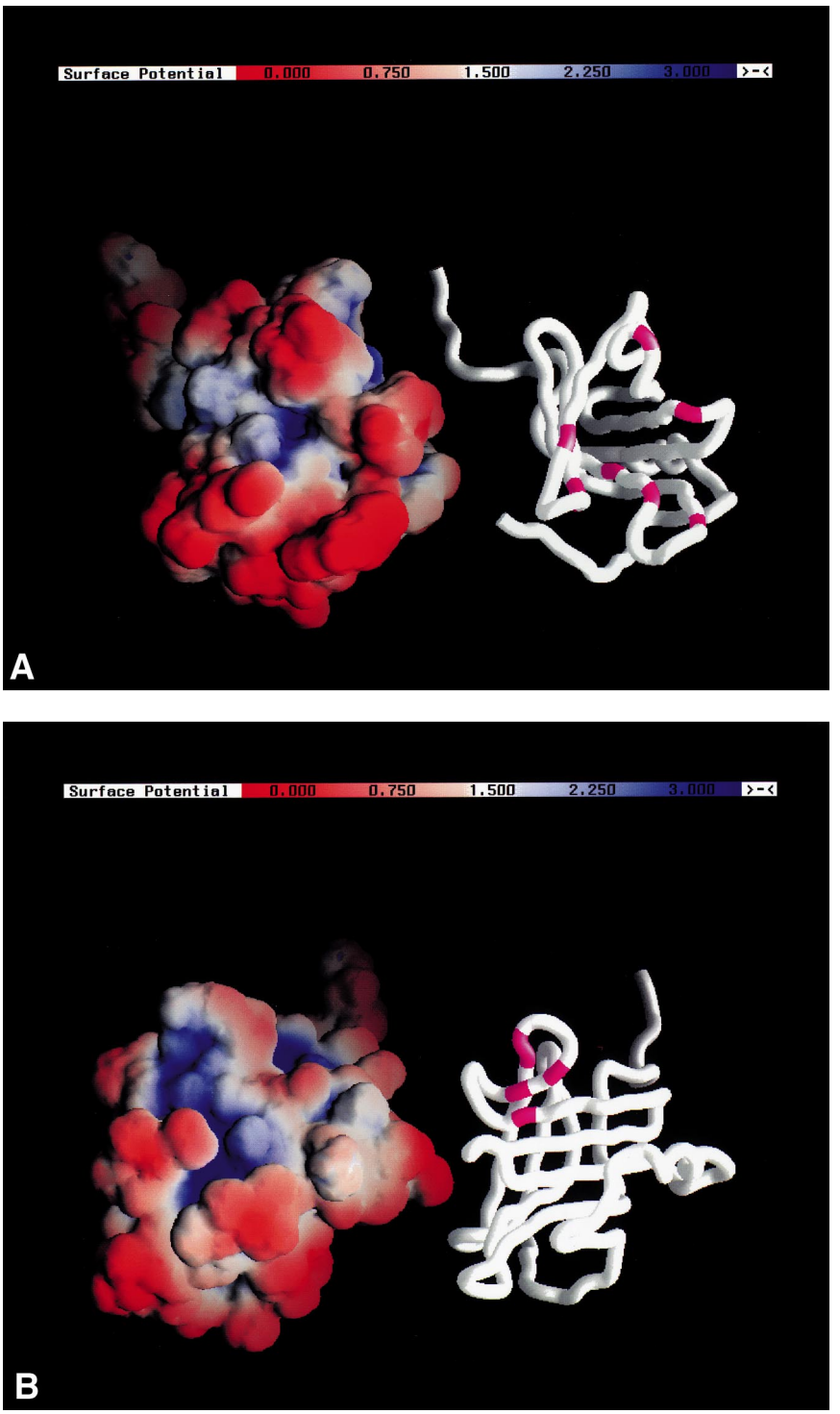

Fig. 5. A: Electrostatic potential at the surface located at the open end of the β-barrel (i.e. at residues 30, 38, 41, 60, 61, 69, 87, 111) shown in the worm representation on the right in purple. The side-chain of residue 61 partly covers, in this particular structure, the high potential region. Electrostatic potential is represented in red at 0.0 kcal/q mol, white at 1.5 kcal/q mol and blue at 3.0 kcal/q mol where q is the protonic charge. B: Same as A for the region located at residues 75, 76, 81, 83, 91.

dues K_{60}, K_{69}, L_{87} is much enlarged and the centre of this region is also within 6 Å from residues S_{30}, P_{38}, V_{41}, W_{61}, A_{111} (Fig. 5). The potential in the region of residues D_{98}, K_{101}, Y_{102}, E_{131}, A_{132}, K_{135} is not among the highest, possibly due to the different orientation of the helix. There are three other high potential spots: two of them involve flexible terminals and one is located at residues K_{75}, T_{76}, V_{81}, K_{83}, K_{91}; (iii) the latter is found at pH 7 on both chains A and B in the dimer where large areas of negative potential are also present. At pH 7 the positive potential region, located at the open end of the β-barrel, is also found in chain A. We retain that this high potential region, less sensitive to conformational details and pH conditions, and possibly one of the regions at the *fg* loop-α-helix interface or at the *de* loop, plays a prominent role in

properly steering negatively charged molecules towards the binding sites.

These findings are consistent with the reported ESMS [24] and fluorescence data (manuscript in preparation), suggesting the presence of more than one binding site for the charged ANS at pH 2. In spite of the difficulties in relating conformational changes with static electrostatic forces, we have observed a substantial upfield shift of the amides belonging to two of these regions, upon increasing the ionic strength and adding 2 M urea, as shown in Fig. 4. The chemical shift variations observed in urea were not due to denaturation, in point of fact, the protein maintains its structure in the presence of 2 M urea, as evidenced from the analysis of NMR NOESY and TOCSY spectra (manuscript in preparation). The effect the added urea has is only to completely shift the equilibrium aggregate ⇄ monomer towards the monomer, in agreement with previously reported data [25]. It is evident from Fig. 4 that the chemical shifts at the *fg* loop-α-helix interface are markedly sensitive to environmental changes in ionic strength and urea concentration. The latter changes could affect electrostatic forces in such a way as to generate a local conformational rearrangement, possibly involving the aromatic side chains of Tyr-99, Tyr-102 and Phe-136, with consequent ring current effects. The same changes could parallel the differences in electrostatic potential in this region between the NMR and X-ray structures.

In summary, we have been able to obtain a structure for the apo form of bovine β-lactoglobulin at pH 2.0 on the basis of data collected by homonuclear ^{1}H NMR spectroscopy only. The monomeric protein at low pH adopts a β-barrel fold, well superimposable on the structure determined by X-ray crystallography for the dimer at physiological pH. NMR evidence points to disordered loop regions and terminal segments. Sizeable differences at the β-barrel-α-helix interface and at the *cd* loop and flanking residues are found within the structured regions. These differences, together with disordering in the loops and in the terminal regions, lead to relevant changes in surface electrostatic properties. However, the high surface potential region at the open end of the β-barrel, which is preserved under disordering and also in the dimer at pH 7, could bear important consequences for the electrostatic steering of negatively charged ligands into the binding site, and the subsequent release of the same ligands, protonated at low pH. The disorder in the *ab* loop, a long Ω loop common to all lipocalins, which has been suggested as forming a lid folded back to partially close the internal ligand binding site [26], could be a prerequisite for ligand release.

4. Supplementary material

Supplementary material includes completed ^{1}H NMR assignment, interproton distance upper bounds and J-couplings and is available upon request.

Acknowledgements: The authors are indebted to Massimiliano Perduca for the purification of several samples, to Fulvia Greco for technical assistance and to Sophie Bevan for carefully reading the manuscript. This work was supported by the Italian National Research Council 'Comitato Biotecnologie' and by the 'Fondazione Antonio De Marco'. This work has been carried out within the framework of EEC concerted action MADGELAS (Contract FAIR-CT96-1202; DG12-SSMI). We gratefully acknowledge the financial support at the Large Scale Facilities of the Frankfurt Biophysik Centre by the European Community's TMR project and Heinz Rüterjans and Frank Löhr for their help and suggestions.

References

[1] Cho, Y., Batt, C.A. and Sawyer, L. (1994) J. Biol. Chem. 269, 11102–11107.
[2] Godovac-Zimmermann, J. (1988) Trends Biochem. Sci. 13, 64–66.
[3] Pervaiz, S. and Brew, K. (1985) Science 228, 335–337.
[4] Ragona, L., Pusterla, F., Zetta, L., Monaco, H.L. and Molinari, H. (1997) Folding Design 2, 281–290.
[5] Molinari, H., Ragona, L., Varani, L., Musco, G., Consonni, R., Zetta, L. and Monaco, H.L. (1996) FEBS Lett. 381, 237–243.
[6] Brownlow, S., Morais Cabral, J.H., Cooper, R., Flowe, D.R., Yewdall, S.J., Polikarpov, I., North, A.C.T. and Sawyer, L. (1997) Structure 5, 481–495.
[7] Townend, R. and Timasheff, S.N. (1960) J. Am. Chem. Soc. 82, 3168–3174.
[8] Narayan, M. and Berliner, L.J. (1997) Biochemistry 36, 1906–1911.
[9] Perez, M.D., de Villegas, D., Sanchez, L., Aranda, P., Ena, J.M. and Calvo, M. (1989) J. Biochem. 106, 1094–1097.
[10] Bax, A. and Davis, D.G. (1985) J. Magn. Reson. 65, 355–360.
[11] Sklenar, V., Piotto, M., Leppik, R. and Saudek, V. (1993) J. Magn. Reson. Ser. A 102, 241–245.
[12] Wüthrich, K. (1986) in: NMR of Proteins and Nucleic Acids, pp. 176–199, John Wiley and Sons, New York.
[13] Güntert, P., Mumenthaler, C. and Wüthrich, K. (1997) J. Mol. Biol. 273, 283–298.
[14] Esposito, G. and Pastore, A. (1988) J. Magn. Reson. 76, 331–336.
[15] Cavanagh, J., Fairbrother, W.J., Palmer III, A.G. and Skelton, N.J. (1996) in: Protein NMR Spectroscopy Principles and Practice, pp. 17–19, Academic Press, New York.
[16] Madura, J.D., Briggs, J.M., Wade, R.C., Davis, M.E., Luty, B.A., Ilin, A., Antosiewicz, J., Gilson, M.K., Bagheri, B., Scott, L.R. and McCammon, J.A. (1995) Comp. Phys. Commun. 91, 57–95.
[17] MacKerell Jr., A.D., Bashford, D., Bellott, M., Dunbrack Jr., R.L., Field, M.J., Fischer, S., Gao, J., Guo, H., Ha, S., Joseph, D., Kuchnir, L., Kuczera, K., Lau, F.T.K., Mattos, C., Michnick, S., Ngo, T., Nguyen, D.T., Prodhom, B., Roux, B., Schlenkrich, M., Smith, J.C., Stote, R., Straub, J., Wiorkiewicz-Kuczera, J. and Karplus, M. (1992) FASEB J. 6, A143.
[18] Nicholls, A. (1993) in: GRASP: Graphical Representation and Analysis of Surface Properties, Columbia University, New York.
[19] Piantini, U., Sorensen, O.W. and Ernst, R.R. (1982) J. Am. Chem. Soc. 104, 6800–6801.
[20] Kim, Y. and Prestegard, J.H. (1990) J. Magn. Reson. 84, 9–13.
[21] Townend, R., Weinberger, L. and Timasheff, S.N. (1960) J. Am. Chem. Soc. 82, 3175–3179.
[22] Honig, B. and Nicholls, A. (1995) Science 268, 1144–1149.
[23] Honig, B. and Yang, A.-S. (1995) Adv. Protein Chem. 46, 27–58.
[24] Hamdan, M., Curcuruto, O., Molinari, H., Zetta, L. and Ragona, L. (1996) J. Mass Spectrom. 31, 1261–1264.
[25] Pace, C.N. and Tanford, C. (1968) Biochemistry 7, 198–202.
[26] Flower, D.R. (1996) Biochem. J. 318, 1–14.